Audio Engineering Society
Convention Paper

Presented at the 118th Convention
2005 May 28–31 Barcelona, Spain

An Accurate Method of Detection and Cancellation of Multiple Acoustic Feedbacks*

Ariel F. Rocha[1] and Aníbal J. S. Ferreira[2,1]

[1] INESC Porto, Porto, Portugal
arocha@inescporto.pt

[2] University of Porto, Portugal
ajf@fe.up.pt, a.j.ferreira@ieee.org

ABSTRACT

This paper presents a new method to the adaptive cancellation of acoustic feedbacks. The method uses high resolution frequency analysis and high-Q notch filters so as to accurately detect feedbacks and cancel them without disturbing noticeably the main audio spectrum. The method will be described, its implementation on a TMS320C6711 DSP platform for real time operation will be explained, and results for the adaptive cancellation of two simultaneous acoustic feedbacks will be presented.

1. INTRODUCTION

The acoustic feedback problem refers to the effect caused by the acoustic coupling between the microphone and the loudspeaker in the same audio amplification system. When that coupling occurs, the amplified sound at the speaker output is propagated back to the microphone and re-amplified.
This closed loop process converts the circuit in an oscillator of audible frequencies and can produce high-pitched whistles ("howling") that interfere with the desired sound and may damage the audio equipment physically [1]. Most common practical solutions applied to the cancellation of acoustic feedback involve the temporary reduction of the amplification gain until the perturbation disappears or the application of a parametric stop-band filter that must be tuned to the feedback frequency whenever it appears. Quite often these methods degrade the quality of the main audio spectrum and their operation requires a time delay that generates perceptual annoyance and increases the risk of equipment damaging.

*This work has been supported by the Portuguese FCT-POSI and European FSE/FEDER research programmes, under project POSI/CPS/48517/2002.

Other proposed solutions try to suppress the feedback disturbances in sound reinforcement systems by applying different techniques based on frequency shifting or phase modulation [1, 2, 3] and, more currently, adaptive microphone arrays [4] and adaptive filtering [5, 6].

When several microphones are activated at the same time, different feedback frequencies can appear simultaneously. Additionally, for fixed microphones the feedback frequency remains constant whereas moving microphones are liable to varying feedback frequencies.

The aim of this paper is to develop an efficient method able to perform a quick and accurate cancellation of multiple simultaneous feedbacks without degrading the main audio spectrum. This method reflects a new feature added to the adaptive equalization system developed in [7].

The paper is organized as follows. In Section 2, the acoustic feedback problem is characterized. Section 3 presents two methods for the automatic suppression of a single sinusoidal interference based on adaptive filtering, which are described and evaluated. Section 4 proposes a new solution for the detection and cancellation of simultaneous feedbacks, based on a high frequency resolution spectral analysis of the audio signal. In Section 5, the implementation for real-time operation of this algorithm is presented and a few results characterizing its performance are documented in Sections 6 and 7. These results are obtained by applying different test signals and creating a real feedback situation. Finally, Section 8 proposes future developments in feedback cancellation, based on the results of this work, and Section 9 concludes the paper.

2. PROBLEM CHARACTERIZATION

The acoustic feedback generation process is illustrated schematically in Figure 1. Based on this Figure, we call *y(t)* the signal captured by the microphone, which is formed by the desired sound signal *s(t)* and the audible disturbance generated by the feedback path *x(t)*. The amplified signal at the sound reinforcement system output is *u(t)*.

Following an analysis similar to that is performed in [1], we call *G* the frequency independent amplifier gain and $F(\Omega)$[1] the Transfer Function (T.F.) of the acoustic feedback path. Consequently, the Source-to-Loudspeaker closed loop T.F. can be written as:

$$\frac{U(\Omega)}{S(\Omega)} = \frac{G}{1 - GF(\Omega)} \qquad (1)$$

The factor $GF(\Omega)$ is called the "open loop gain" of the system.

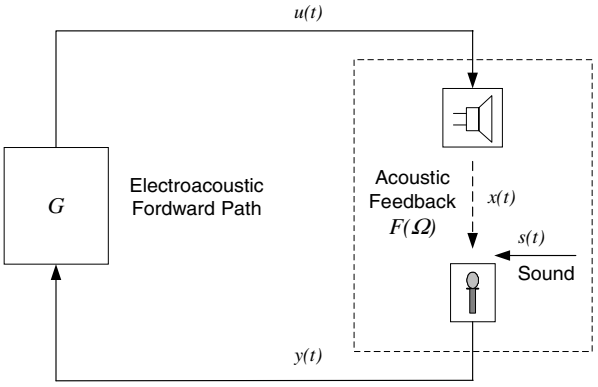

Figure 1: Schematic of an audio amplification system producing acoustic feedback.

The closed loop system will remain stable if the open loop gain is $|GF(\Omega)| < 1$ at all angular frequencies. If the amplifier gain is gradually increased, then the quantity $|1 - GF(\Omega)|$ could become very small for certain frequencies, at which the absolute value of the closed loop T.F. will be significantly increased. Then, the system will become unstable generating self-excited oscillations which result in strong whistles characterized by a narrow bandwidth and a prominent peak in the spectrum.

[1] In this paper, we use the symbol Ω to represent the continuous angular frequency, in place of the character employed in the referred bibliography [1], and the symbol ω is used to represent the discrete angular frequency.

In order to apply an automatic method of acoustic feedback suppression that avoids delays and audio spectrum degradation, two solutions can be considered:

I) Parametric Notch Filtering:

Suppresses the narrow band oscillations originated from the system instability. The notch filter is tuned to the frequency of the interference whenever such instability occurs.

II) Adaptive Cancellation:

Estimates the feedback signal *x(t)* by recursively identifying and tracking the feedback path Transfer Function *F(Ω)* (which is unknown). Then, the interference is cancelled by subtracting *x(t)* from the input signal.

3. ADAPTIVE SOLUTIONS FOR SINGLE FEEDBACK CANCELLATION

The first objective of this work was to apply the concept of adaptive cancellation in the automatic suppression of interferences produced by acoustic feedback, studying its behavior and evaluating the results. The use of a FIR or IIR structure for the filter determines its connection to the sound reinforcement system and the way the interference cancellation is performed. On the other hand, the computation of each type of structure exhibits certain special features that are presented in the next subsections.

3.1. Adaptive FIR Filter Solution

This method tackles the feedback suppression problem as an acoustic echo cancellation problem by using a FIR filter. Figure 2 displays a schematic of the circuit in the discrete-time domain. The main goal is to generate a T.F. opposite to that is produced by the speaker-microphone interaction, in order to cancel the interference component received by the microphone. In order to achieve this, the FIR filter is connected in parallel with the electro-acoustic path. For the adaptive filtering, a transversal filter is used, whose tap weights are adapted by means of an adaptive procedure such as the Least-Mean-Squares (LMS) algorithm [8].

The FIR filter uses a reference input, *u(n)*, so as to generate, at its output, an estimation of the sinusoidal interfering signal contained in the primary input, *d(n)*.

Thus, the filter will produce an output signal, *y(n)*, which, once subtracted to that coming from the microphone, will eliminate or, at least, strongly attenuate the interference.

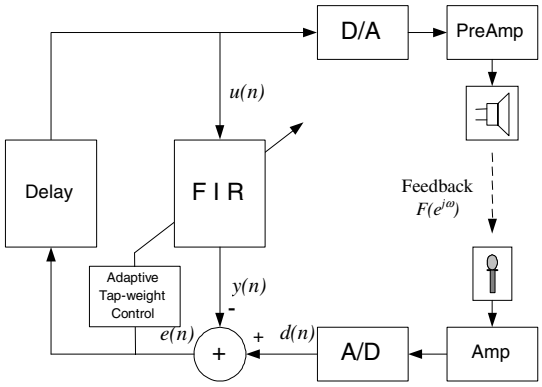

Figure 2: Adaptive FIR filtering applied to cancel acoustic feedback.

The FIR filter length (total number of tap weights) must be proportional to the time delay caused by the propagation of the acoustic signal on the air (between speaker and microphone), in order to make the subtraction between signals with effective alignment in time.

The adaptive FIR-based algorithm for cancellation of sinusoidal interferences was implemented on the TMS320C6711 DSP platform [9] for real time evaluation. The code creates a FIR filter of length 32 and uses the normalized LMS (NLMS) adaptation algorithm [8]. This method, unlike the LMS, allows us to make the adaptation independent of the input signal maximum amplitude. Input signals *d(n)* and *u(n)* were generated as vectors.

As a result of the DSP implementation test, a set of "learning curves" (that means, curves of convergence to zero of the Mean Squared Error, MSE) were obtained by monitoring the evolution in time of *e(n)*, for different values of the adaptation step size parameter μ [8], covering the entire audio frequency spectrum. Figure 3 shows a set of learning curves for different frequencies using a step size of $\mu = 0.001$.

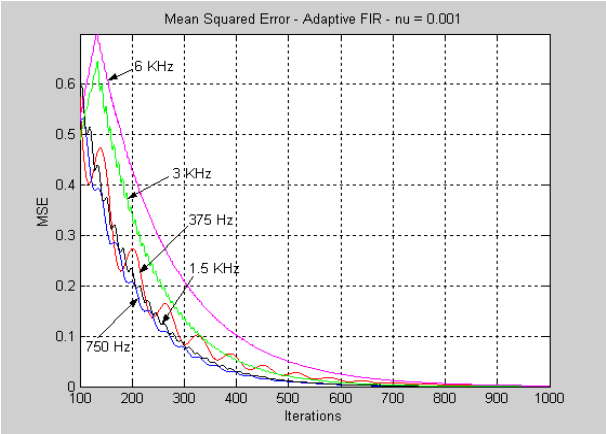

Figure 3: Learning Curves of the Adaptive FIR filter implemented on DSP, with $\mu = 0.001$, for different test frequencies.

As can be seen in Figure 3, the performance of the algorithm is approximately the same, for all frequencies analyzed in the simulation, monotonously reaching the region of convergence before 1000 iterations for every case. Only an increasing ripple is observed at lower frequencies. Keeping the test frequency constant, it was verified (as we expected) that the lower the value of μ the slower is the convergence of the MSE. Because of the use of a FIR filter (a Moving Average structure [10]) the system reveals an inherent stability.

3.2. Adaptive IIR Filter Solution

This method combines the two approaches mentioned in section 2, applying an adaptive notch filter, which tracks the interference and suppresses it automatically. A second order IIR structure is used to implement the notch filter. The corresponding circuit diagram is presented in Figure 4. The IIR filter is connected in series to the electro-acoustic path, processing the signal coming from the microphone in a multiplicative manner.

By definition, a Notch filter attenuates frequencies in a narrow bandwidth around the cut-off frequency. Therefore, its Transfer Function must have a zero in the central frequency in order to create a (theoretical) null at this point in the frequency response characteristic.

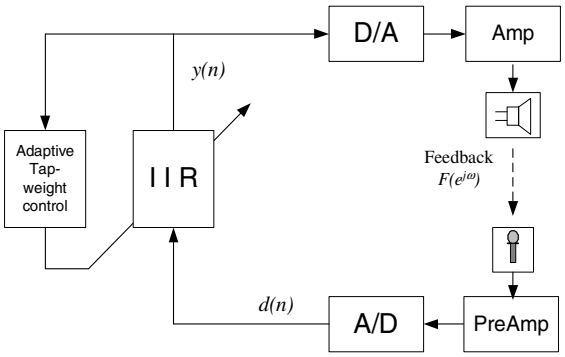

Figure 4: Adaptive IIR filtering applied to cancel acoustic feedback.

The narrow bandwidth condition can be reached by introducing a pole in the vicinity of the zero. This produces a resonance in the environs of the null and thus reduces the notch bandwidth. Hence, one possible way to implement a notch filter is performing a system having the following T. F. in z domain [10]:

$$H(z) = b_0 \frac{1 - 2\cos(\omega_0) z^{-1} + z^{-2}}{1 - 2r\cos(\omega_0) z^{-1} + r^2 z^{-2}} \qquad (2)$$

Where ω_0 is the notch angular frequency: $\omega_0 = 2\pi f_0$.
Eq. (2) has a pair of complex-conjugate zeros on the unit circle at an angle ω_0, that is:

$$z_{1,2} = e^{\pm j\omega_0}$$

It also presents a pair of complex-conjugate poles at:

$$p_{1,2} = re^{\pm j\omega_0}$$

From the previous equations, we observe that r establishes the ratio between the modules of the pole and the zero of $H(z)$ (or, in other words, it is the pole module normalized to the zero module value). Therefore, that parameter has a direct influence on the notch bandwidth and the notch depth (the attenuation at the central frequency of the notch). Consequently, if the parameter r increases, the notch bandwidth becomes narrower and the notch depth decreases.

In order to obtain a stable system, it must be observed that: $r < 1$. As an example, Figures 5 and 6 present the zero-pole model of $H(z)$ and the frequency spectrum of a Notch filter defined by Eq. (2), with $f_0 = 6000$ Hz and $r = 0.7$.

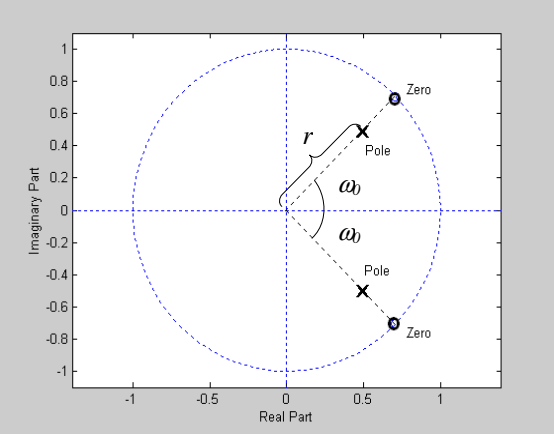

Figure 5: Zero-pole pattern of the Notch Filter Transfer Function

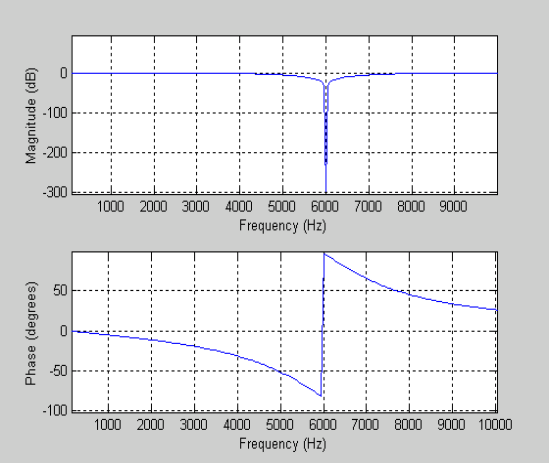

Figure 6: Notch Filter frequency response, including Magnitude (above) and Phase (below) curves.

Similarly to what was previously done with the FIR filter model, we performed the evaluation of the adaptive IIR filter model by implementing the algorithm on the already mentioned DSP platform.

The general expression of the second order IIR filter Transference Function is:

$$\frac{Y(z)}{U(z)} = \frac{b_0 + b_1 z^{-1} + b_2 z^{-2}}{1 + a_1 z^{-1} + a_2 z^{-2}} \qquad (3)$$

In this particular case, Eq. (3) must be corresponding to a notch filter, so we can rewrite as:

$$\frac{Y(z)}{U(z)} = \frac{1 + b_1 z^{-1} + z^{-2}}{1 + a_1 z^{-1} + r^2 z^{-2}} \ , \qquad (4)$$

where:

$$b_1 = 2\cos(\omega_0) \qquad (5)$$

$$a_1 = 2r\cos(\omega_0) = rb_1 \qquad (6)$$

The second order IIR filter is implemented by means an AR-MA process [8, 10]. However, the tap-weight adaptation is performed by applying the NLMS method only in the MA part of the structure, in order to reach an asymptotic convergence without stability problems.

The one tap-weight adapted by the algorithm is b_1, which modifies also the value of a_1, by means of the fixed relation established by r, as it is expressed by Eq. (6). This is necessary in order to maintain the notch bandwidth constant. Coefficients b_0, b_2 and a_2, keep always in their prefixed values. The algorithm uses the NLMS method to perform the adaptation process.

Due to the AR part of the IIR model, which adds poles to the Transfer Function, the computation of the adaptive filter tends to instability if its coefficients are not restricted in magnitude by the adaptation process. This is due to the fact that, from Eq. (5), b_1 is restricted by the following limits:

- $\omega_0 = 0 \rightarrow b_1 = 2$
- $\omega_0 = \pi \rightarrow b_1 = -2$

In the adaptive IIR filter implementation, if due to the adaptation process, b_1 varies without any restriction on its magnitude, it could happen that, at some frequencies and for certain values of μ, its module becomes greater than 2. This forces the location of the zero to go out of the unitary circle in the z plane (see Figure 5). The variation of b_1 produces a subsequent variation of a_1, which defines the module of the pole at z^{-1}. Therefore, this coefficient could also go out of the unitary circle, causing the filter output to grow indefinitely, that is, the system instability. This effect can take place specially at low frequencies near to $\omega_0 = 0$ or high frequencies near to $\omega_0 = \pi$, for which the module of b_1 approaches to 2. In order to solve this stability problem, the algorithm performs a monitoring of the tap-weight b_1 and limits its value so that it is constrained between –2 and 2.

Figure 7 shows a set of learning curves of the adaptive IIR notch filter, obtained on real time implementation for different frequencies, with a zero-pole relation of r = 0.8 and using an adaptation step size μ = 0.01.

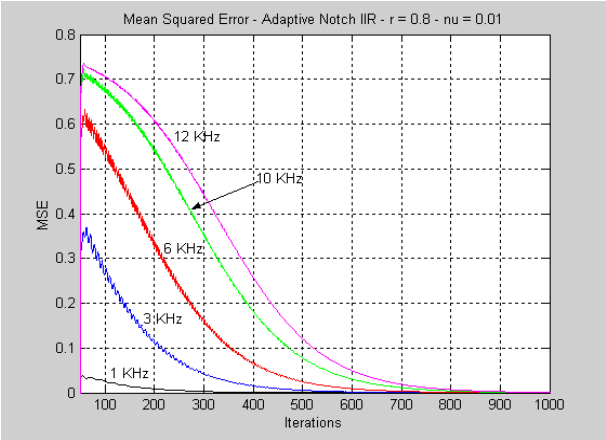

Figure 7: Adaptive IIR filter learning curves for different frequencies, with μ = 0.01 and r = 0.8.

As a result of the supervision and restriction of the value of b_1, the filter is stable and exhibits a quick but soft convergence under 1000 iterations in all cases.
In this model, we need that the notch bandwidth be as narrow as possible, in order to cancel only the feedback signal (that is similar to a pure sinusoidal tone) but without attenuating other desirables components of the main audio spectrum that can be near in frequency to the feedback. For this reason, the parameter r should be as close as possible to 1. On the other side, it can be concluded from the obtained learning curves that, when the interfering frequency is higher than 6 KHz, the convergence becomes slower for values of r over 0.8. Hence, a compromise value must be found for this parameter.

3.3. Remarks and Conclusions about Adaptive FIR and IIR Methods

From the test results we conclude that, by choosing conveniently the value of μ for the notch IIR filter model, it is possible to obtain approximately the same speed of convergence than for the FIR model. Then, the adaptive notch IIR model represents a good solution to cancel adaptively a sinusoidal interference, because it has a less computational cost than the FIR model.

Adaptive filtering techniques represent an efficient solution for the single acoustic feedback case and they are proposed, with different approaches, in various papers related specially to hearing aids [11, 12, 13].

In the two presented algorithms, the interfering signal is tracked in the time domain in order to be identified and removed. In presence of two or more perturbations, both algorithms exhibit an inherent difficulty in deciding which one must be cancelled. Consequently, those methods are not effective when several feedbacks are present simultaneously.

4. ALGORITHM FOR DETECTION AND CANCELLATION OF MULTIPLE FEEDBACKS

For simultaneous feedbacks cancellation, this paper proposes a new solution based on a high frequency resolution spectral analysis of the audio signal.

4.1. General Concepts

The main idea is to obtain a high-resolution spectral representation of the digitalized acoustic signal and then analyze it, bin by bin, in order to detect the spectral peaks that indicate the presence of feedback. The spectral peaks are identified based on the geometric shape of their spectra. Then, a criterion is applied in order to decide if they correspond to feedbacks or desired components of the acoustic signal. In order to cancel the perturbations, a set of high-Q notch filters, implemented by using a second order IIR model, is arranged. When feedback peaks are detected, their frequency are estimated accurately and the notch filters' tap-weights are set. Thus, a notch filter is precisely placed at the central frequency of every feedback.

In this case, the algorithm does not perform an iterative adaptation of filers' tap-weights (sample by sample), but the spectrum is analyzed for every new received frame in order to keep or modify the parameters of the applied notch filters.

In Figure 8 we can see a block diagram of the general process, covering the digitalized signal path, the notch filtering, the technique applied for feedback detection and the filters' tap-weights setting. Once the acoustic signal coming from the microphone *s(t)* is sampled, the discrete time signal *x(n)* is obtained.

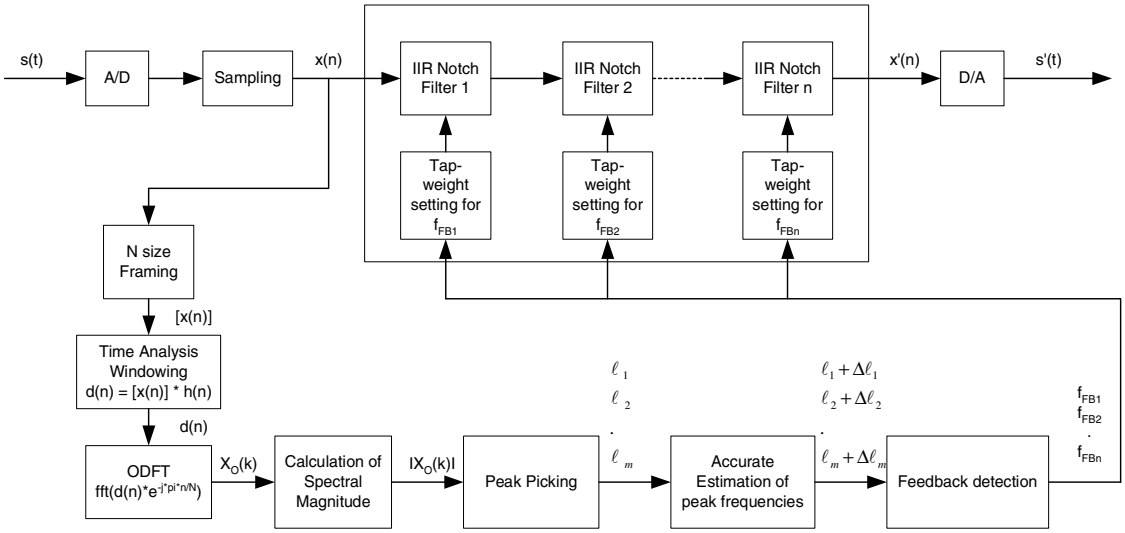

Figure 8: General Algorithm of the Multiple Feedbacks Canceller.

Then, the algorithm takes frames of N = 1024 samples, applying a sinusoidal time windowing on them and computes the Odd Discrete Fourier Transform to represent the spectrum. As a result of the process of detection of feedbacks performed on the discrete spectrum, the feedback frequencies (if any) are calculated (f_{FB1}, f_{FB2},…, f_{FBn}) and a bank of notch filters is applied to *x(n)* in order to suppress the interferences. Thus, the discrete filtered output signal *x'(n)* is returned by the algorithm and converted to the continuous time domain by the A/D converter. The analogue output signal is identified in the block diagram as *s'(t)*.

4.2. ODFT Analysis

As was already mentioned, the Odd DFT (or simply ODFT) is applied on the discrete time input signal in order to perform its conversion from time domain to frequency domain. There are several reasons that justify the use of this transform, which are related to:

- computational efficiency,
- transform symmetry convenience [14],
- the fact that the ODFT is the analysis/synthesis scheme used by the 20 bands adaptive equalizer main program, in which the feedback canceller will be integrated as new feature [7].

For the input discrete time signal generically expressed as *x(n),* the expression of the ODFT is:

$$X_O(k) = \sum_{n=0}^{N-1} h(n).x(n).e^{-j\frac{2\pi}{N}\left(k+\frac{1}{2}\right)n} \qquad (7)$$

Where *h(n)* is a real function that represents the time analysis window of length *N* and determines the basic analysis framework for *x(n)*. Different functions can be adopted for the window according to the most convenient spectral shape, but generally observing the condition of being real, symmetric and with a size that depends on the nature of the analyzed signal.

The developed algorithm uses the same analysis scheme implemented in [7], applying a window *h(n)* of length *N*=1024 elements to perform the time windowing of *x(n)* and obtaining a discrete *N*-sized frame. Then, in order to obtain the ODFT coefficients, the whole frame is multiplied by the exponential function $e^{-j\frac{\pi}{N}n}$ and the *N*-sized Fast Fourier Transform is computed. This process allows us to obtain a real frequency spectrum of *N*/2 bins from the input audio signal.

4.3. Peak Picking

The so called "Peak Picking" method is used to detect the spectral peaks present in the audio signal spectrum. This is performed by calculating the magnitude in dB of the ODFT spectrum for the current frame. Then, the algorithm detects the local maxima of the spectrum and selects, among these maxima, those which have the shape of spectral "peaks".

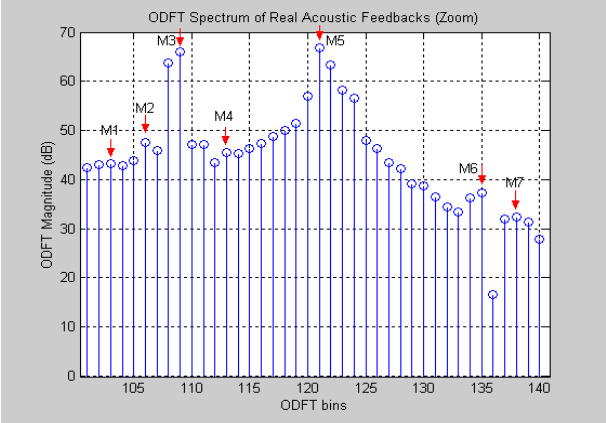

Figure 9: Partial view of the ODFT spectrum corresponding to an audio signal containing feedbacks. Local maxima are signaled.

Figure 9 shows part of the 512 bin-spectrum corresponding to a sampled audio signal frame that presents two real acoustics feedbacks. By applying the Peak Picking method to analyze the spectrum, seven maximum bins are found in the displayed fraction, which are identified in Figure 9 by: "M1", "M2",…, "M7". The maxima corresponding to the spectral peaks are M3 (bin 110) and M5 (bin 121).

It should be noticed that the magnitude of a local maximum directly influences on the performance of the algorithm. A level too low could produce false detections whereas a level too high could lead to ignore some real peaks. Thus, a suitable tradeoff must be carefully set in order to avoid erroneous detections.

4.4. Accurate Frequency Estimation

One of the main goals of the present work is to remove feedbacks applying the notch filtering in every exact feedback frequency, without degrading the adjacent audio spectrum. To make this effectively, the exact estimation of detected peaks frequency is essential.

For this reason, an accurate estimation algorithm is applied to calculate the spectral peak frequencies, obtaining the integer and fractional parts of those values. This algorithm was developed in [14]. In the following paragraphs, a brief resume of the principal concepts applied by this method will be presented.

We can consider a discrete sinusoid defined by:

$$x(n) = A.\sin\left[\frac{2\pi}{N}(\ell + \Delta\ell).n + \Phi\right] \qquad (8)$$

where A is the magnitude, ℓ and $\Delta\ell$ are respectively the integer part and the fractional part of a DFT-type frequency bin scale. N is the discrete time period, in number of samples, and Φ is the initial phase.

In order to obtain the ODFT defined by Eq. (7), the referred paper [1] proposes the following time analysis window:

$$h(n) = \sin\frac{\pi}{N}\left(n + \frac{1}{2}\right) \;;\; 0 \le n \le N\text{-}1 \qquad (9)$$

This sine window represents the square root of a shifted *Hanning* window, and its frequency response is obtained from:

$$H(\omega) = \sum_{n=0}^{N-1} h(n).e^{-j\omega n} \qquad (10)$$

whose result is:

$$H(\omega) = \frac{\cos\left(N\frac{\omega}{2}\right)}{2}\left[\frac{1}{\sin\frac{1}{2}\left(\frac{\pi}{N} - \omega\right)} + \frac{1}{\sin\frac{1}{2}\left(\frac{\pi}{N} + \omega\right)}\right]. \qquad (11)$$

From Eq. (11), it can be verified that $|H(\omega)|$ is a low-pass filter with a main lobe (the pass-band) whose width is $\frac{6\pi}{N}$ and a stop-band envelope that monotonously decreases and exhibits zeros at:

$$\omega = \pm\left(\frac{\pi}{N} + k\frac{2\pi}{N}\right), k = 1,2,3,...$$

Each channel of the ODFT filter bank is obtained by modulating *H(ω)* to the discrete center frequencies:

$$\omega = \pm\left(k+\frac{1}{2}\right)\frac{2\pi}{N}, k = 0,1,...,N-1$$

As was explained and demonstrated in [14], a sinusoid which frequency is $\omega = \frac{2\pi}{N}\ell$, where ℓ is an integer value, will be "seen" by the frequency responses of two ODFT channels whose indexes (*k*) are $\ell-1$ and ℓ. For the case of a sinusoid whose frequency is not just discrete but generally given by $\omega = \frac{2\pi}{N}(\ell + \Delta\ell)$ with $1 \le \ell \le \frac{N}{2}-1$ and $0.0 \le \Delta\ell < 1.0$, it will be represented by at least two sub-bands below the Nyquist frequency.

Given that the magnitude of sub-band $k = \ell$ of the ODFT filter bank will be a local maximum, the value of ℓ can be directly obtained from the ODFT spectrum and the fractional frequency $\Delta\ell$ can be calculated by using the relative magnitudes of sub-bands $k = \ell - 1$ and $k = \ell + 1$.

Considering the applied analysis window *H(ω)*, it can be demonstrated that a good approximation for the fractional part of the frequency is given by [14]:

$$\Delta\ell \cong \frac{3}{\pi}\arctan\frac{\sqrt{3}}{1+2\left[\frac{|X_O(\ell-1)|}{|X_O(\ell+1)|}\right]^{1/G}} \qquad (12)$$

The constant *G* in Eq. (12) has been set to an adequate value of 27.4/20.0, but it can be adjusted to other values in order to minimize the maximum absolute error of the estimation. As it will be verified by the test results, the absolute frequency estimation error is less than 1%.

With respect to the algorithm displayed in Figure 8, the accurate values (expressed in bins) obtained for every estimated frequency, are designed by the pairs $(\ell_1 + \Delta\ell_1)$, $(\ell_2 + \Delta\ell_2)$, etc, where ℓ is the integer part of the frequency and $\Delta\ell$ is the fractional part of every found feedback frequency.

4.5. Feedback Detection

In order to determine if the detected peaks are produced by feedback, two rules are considered by the developed algorithm.

The first rule considers the relation between the energy of the every single peak and the whole spectrum energy. The ratio between these two magnitudes is matched against a threshold (that we will call *ENERGY_THRESHOLD*) in order to decide whether the peak is likely to reflect a feedback or not.

With the aim of calculating the energy of the input signal for the current frame, we recall the Parseval´s relation that expresses the energy of a discrete-time signal *x(n)* in terms of its spectral characteristic *X(ω)*. By applying this concept to a discrete-time signal with finite energy, its energy is defined as [10]:

$$E_x = \sum_{n=-\infty}^{\infty}|x(n)|^2 = \frac{1}{2\pi}\int_{-\pi}^{\pi}|X(\omega)|^2 d\omega \qquad (13)$$

where $|X(\omega)|^2$ is the *energy density spectrum* of *x(n)*. Power signals do not have finite energy and are characterized by its *power density spectrum*.

Considering the symmetry property of the ODFT [14] and the periodicity of its time and frequency representation, the algorithm computes the power spectrum of the discrete-time audio input signal from the *N*/2=512 bins corresponding to its discrete spectral representation *X(k)*, and obtains the frame total power, as follows:

$$P_x = \sum_{k=0}^{\frac{N}{2}-1}|X(k)|^2 \qquad (14)$$

In order to compute the energy of the spectral peaks, the squared magnitudes corresponding to the considered maximum bin and two adjacent bins at both sides are added:

$$E_p = \sum_{k=b_M-2}^{b_M+2}|X(k)|^2 \qquad (15)$$

Where: b_M is the examined maximum bin number.

Hence, the condition can be stated in the following way:

$$\frac{P_x}{E_p} < ENERGY\_THRESHOLD \quad (16)$$

If the energy of the spectral peak is as strong as for the condition of Eq. (16) be observed, then the algorithm decides that the peak is "suspicious" of feedback. Otherwise, the peak is considered as a normal component of the audio signal.

The value of *ENERGY_THRESHOLD* influences the sensitivity of the algorithm in recognizing the feedback peaks. Increasing this parameter allows a quick detection of spectral peaks but can produce more false detections whereas a low threshold implies a slower but more secure identification of peaks.

The second rule considered is the feedback property of stationary frequency in opposition to the varying frequency components of human voice or musical instruments. When the same suspicious peak appears continuously for a certain number of frames, the probability of being produced by feedback is high.

It is well known that the integration period of the human ear is approximately 50 ms. That period is the maximum time that the canceller can invest in order to identify and suppress a new feedback interference, before it is listened. Since the sampling frequency of the system is 48000 Hz, the time to complete the spectral analysis of every new frame (making a new detection) is 10.7 ms [7]. Thus, by comparison of this time with the human ear integration period, we conclude that the feedback detection method can consider up until 4 consecutive detections of the same new spectral peak in order to track it without audible perception. The developed algorithm considers that if the same spectral peak is detected for 3 consecutive times, it is produced by acoustic feedback.

When several continuous peaks are detected simultaneously, the accurate frequencies of the *n* highest ones are registered and *n* notch filters are set from those values in order to cancel the interferences. The developed algorithm was tested for two simultaneous feedbacks. However, the method can be applied in order to detect and suppress a higher quantity of simultaneous interferences.

4.6. High-Q Notch Filtering

In order to remove the detected feedbacks, a bank of highly selective notch filters is applied to the processed signal. Their high selectivity allows filters to be applied in the exact feedback frequencies without degrading the adjacent spectrum.

The selectivity of a stop band filter can be expressed by the Quality factor, which relates the central frequency and the bandwidth of the stop band. For a notch filter, the Quality factor, or simply *Q*, is obtained by dividing the center frequency of the notch by the -3 dB bandwidth of the filter, as follows:

$$Q = \frac{fc_{Notch}}{B_{-3dB}} \quad (17)$$

Regarding the *Q* factor, we can consider two options. The first one is to keep constant the value of *Q* along the spectrum, by modifying the filter bandwidth in accordance to the notch frequency.

The second alternative is to keep the notch bandwidth constant along the spectrum. In the present work, the second option is performed. As a consequence, the filter *Q* will vary according to the notch frequency in a directly proportional manner, increasing its value for higher frequencies. However, in order to observe the high selectivity constraint for the whole frequency spectrum (even at lower frequencies), an adequate value for *r* was chosen, to rise a *Q* factor equal to or higher than 10 at 10 KHz. As it was verified experimentally, in order to observe this condition, an adequate value of *r* should be equal or higher that 0.93.

According to the results obtained with the second order IIR filter model and taking account into its low computational cost, this structure was selected to implement the Notch filters applied to suppress the interferences produced by multiple feedbacks.

5. REAL TIME OPERATION

The presented algorithm for multiple feedbacks cancellation was implemented for real-time operation, using the previously applied TMS320C6711 DSP platform [9]. The DSP code was written in C language and reutilizes the main code previously developed for the 20 bands adaptive equalizer [7].

Experimental tests have indicated that best results were obtained using for *ENERGY_THRESHOLD* the value of 10 dB and this is the setting for the implementation.

With the aim of evaluate different aspects of the performance of the algorithm, several tests were performed applying different input signals. For a first evaluation, an audio test signal was applied to the system input, composed of audible pure tones added to a musical background. This background serves to evaluate the influence of the canceller on the main audio spectrum. The audio tones and the musical background were generated digitally in a PC.

Next, a sound reinforcement system was built and the canceller was evaluated in a real feedback situation. Results of the mentioned tests are presented in following sections.

6. TEST WITH TWO SIMULTANEOUS SINUSOIDS

In order to have a concrete evidence about the ability of the implemented algorithm to track and cancel simultaneous variable frequency interferences, two sinusoids of modulated frequency, f_{c1} and f_{c2}, with a different modulating frequency for each one (f_{mod1} and f_{mod2} respectively), were applied simultaneously to the system input, over the music background.

Input Test Signal 1:

- f_{c1} = 5100 Hz
- f_{mod1} = 1 Hz
- Maximum deviation of f_{c1} = 200 Hz

Input Test Signal 2:

- f_{c2} = 3100 Hz
- f_{mod2} = 2.5 Hz
- Maximum deviation of f_{c2} = 200 Hz

Music Background: wav file

Graphs of frequency vs. time ("specgram") were obtained for both input and output signals, which are presented in Figures 10 and 11, respectively. In such figures, it can be noticed that the algorithm closely tracks the frequency variations of the test sinusoids, and attenuates them considerably.

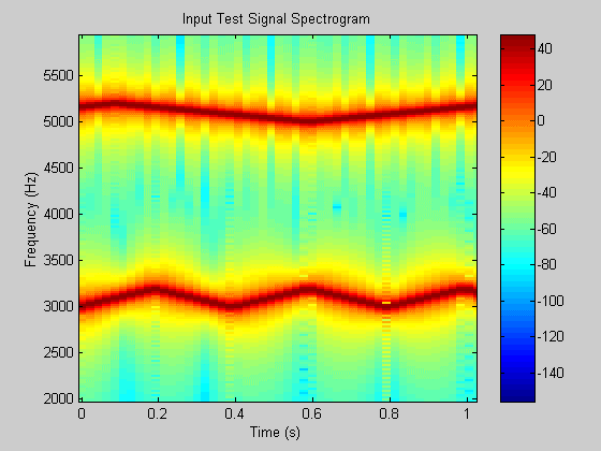

Figure 10: Input signal spectrogram for two simultaneous variable frequency test sinusoids.

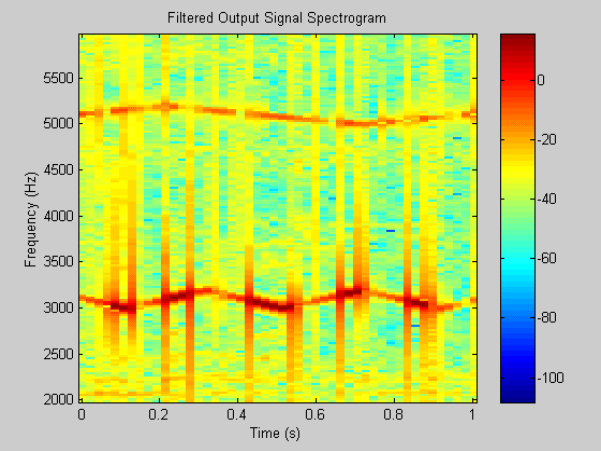

Figure 11: Output filtered signal spectrogram for two simultaneous variable frequency test sinusoids.

The DSP development environment used for the implementation (Texas Inst. "Code Composer") incorporates a signal analysis interface that is able to display signal data. This feature was applied to obtain instantaneous views of the processed signals in the frequency domain. (To obtain those graphs, the DSP code execution must be stopped).

By using that visual tool, Figure 12 shows the input test signal spectrum in which the spectral peaks of the two moving sinusoids can be clearly observed at the regions of 3 KHz and 5 KHz, respectively. In the same way, the output filtered signal spectrum is depicted in Figure 13. In both cases, the spectral magnitude is presented in a logarithmic scale and the two spectra were obtained at the same code breakpoint.

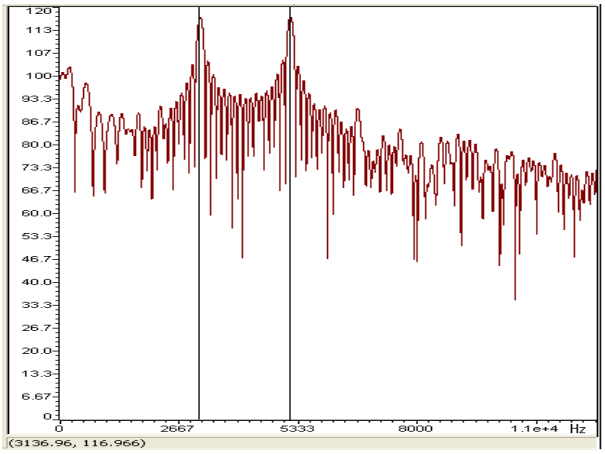

Figure 12: Input Signal Spectrum with two simultaneous variable frequency test sinusoids.

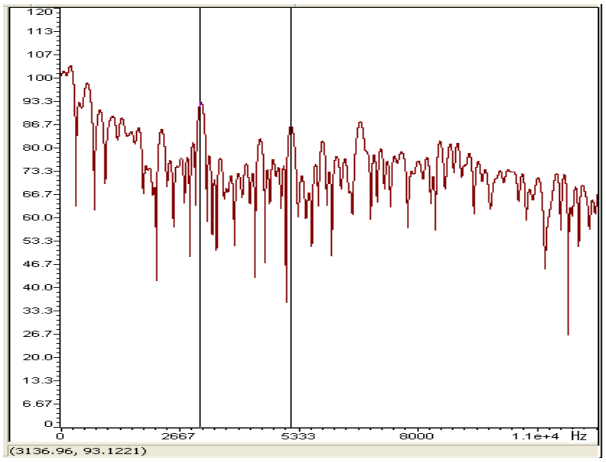

Figure 13: Filtered Output Signal Spectrum for two simultaneous variable frequency test sinusoids.

Comparing the input and output spectra, it can be observed, once more, a strong attenuation (that we can visually estimate near to 25 dB) at the central frequency of every interfering peak, preserving the shape of the main spectrum.

Although a noticeably attenuation of the test signal spectral peaks is achieved, we can observe in Figure 13 that those peaks are still present in the spectrum of the filtered output signal. This is due to the artificial condition created by the application of test signals in a permanent manner at the system input, which is quite different from a real situation of acoustic feedback. Under such real conditions, it is possible to appreciate that when the notch filtering is applied at the precise frequency of the interference, the positive feedback closed loop is interrupted for that frequency and the disturbance tends to disappear while the filter is active.

Since the internal storage registers used by the DSP code can be shown by the graphic interface of the development environment, the calculated frequency value for the detected peak can be directly read from the PC display. Using this possibility, we verified that the frequency estimation error lies between 0.1% and 0.2%.

The obtained results allow us to verify the high accuracy of the algorithm in the frequency estimation and its ability to track the applied moving frequency sinusoid signals.

7. TEST WITH REAL FEEDBACKS

The circuit shown in Figure 14 was implemented with the purpose of create two simultaneous feedback loops, each one produced by the coupling between one loudspeaker and one directional microphone placed in its proximity. These loops are generated in the same sound amplification path, in the middle of which the feedback canceller is inserted.

After several attempts with different layout of the equipment, two feedback signals were obtained at the same time as a consequence of increasing the main amplification gain. The feedback peaks were separated in the spectrum although with nearby frequencies. This condition was achieved several times in a repetitive mode, thus generating a double interference in a controlled way.

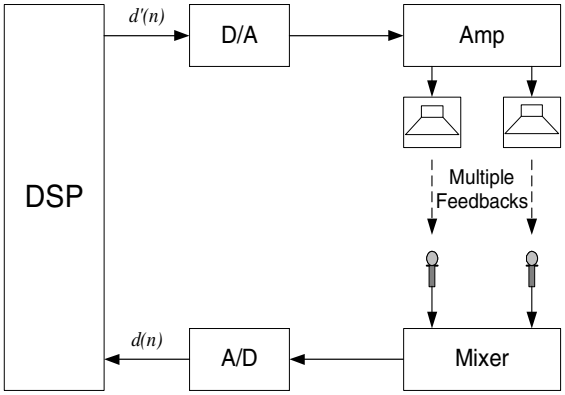

Figure 14: Double Acoustic Feedback generated by means two simultaneous couplings.

The feedback canceller was activated in this context, exhibiting its ability to quickly detect and attenuate the generated interferences, preventing their growth in amplitude. A similar result was verified when one of the microphones was forced to move around its original position, with the purpose of vary the feedback frequency. A similar test was performed using one microphone to pick up a speech, while simultaneously the other one was generating a feedback. It was verified again an acceptable suppression level of the interference with a very small or negligible alteration of the quality of the voice. These last observations are based on the subjective appreciation of expert listeners.

7.1. Remarks on parameters' setting

Acoustic feedback can be produced in different sound reinforcement contexts, as for example live music amplification during a concert or speech amplification used for lectures (public address). In the first case, there exists a greater probability of false detections due to the number of spectral components of the music with a shape similar to a feedback peak. This implies to consider a higher value for the peak energy in the first mentioned feedback detection rule (setting a lower value of *ENERGY_THRESHOLD*), in order to identify just the true feedbacks, responding less to desired sounds. Nevertheless, for speech-only applications, it is necessary a higher detection sensitivity so as to detect and remove feedbacks more quickly. This can be accomplished by setting a higher value of *ENERGY_THRESHOLD*.

When the acoustic feedback is produced by fixed microphones (typically, during the sound checking previous to an event), the effect is more extended in time, usually keeping the whistle pitch constant. This requires that the notch filtering remains activated until the cause of the interference is eliminated (By modifying the location of loudspeakers, microphones, etc). On the other hand, when the feedback is produced by mobile microphones during a performance, its generation is more abrupt and the audible effect is instantaneous, with the possibility of whistles of variable pitch. This makes necessary that the filters can be quickly activated, tracking the interferences, and then automatically deactivated in a short time.

8. FUTURE DEVELOPMENTS

Depending on the environment and situation in which a feedback cancelling system that uses the present algorithm is applied, it could be necessary to set it in different operation modes. From the satisfactory results obtained with the developed method in detection and suppression of two simultaneous feedbacks, the suggested next step for future developments in the short term is to adapt the current algorithm in order to perform the cancellation of a larger number of multiple feedbacks (for example, more than 12 simultaneous interferences) so as to improve the standards of the existing commercial equipments. This requires a flexible setting for the parameters and notch filters operation mode, according to the different mentioned situations. Then, an optimized version of the DSP code should be integrated to the 20 bands adaptive equalizer main program as another feature added to that sound processing system.

The previous results also pave the way to the controlled insertion of probe sinusoids that can be used to perform automatic and transparent equalization of rooms. This is an important future development.

9. CONCLUSION

In this paper, we have presented a new method for accurate detection and cancellation of multiple acoustic feedbacks that combines techniques for precise spectral identification of simultaneous interferences and narrow notch filtering. From the different tests performed with simulated sinusoidal interferences and real acoustic feedbacks, it was demonstrated that the developed algorithm is able to detect quick and accurately two simultaneous feedback peaks applying a precise notch filtering to each one in order to strongly attenuate their disturbance.

10. REFERENCES

[1] Heinrich Kuttruff (with the contribution of David Highfield), "*Room Acoustics",* 4th. Edition, Spon Press, London, New York, 2000 (obtained from the Taylor & Francis e-Library, 2001).

[2] M. R. Schroeder, *"Improvement of acoustic-feedback stability by frequency shifting"*, Journal of the Acoustical Society of America, vol. 36, no. 9, 1964.

[3] J. L. Nielsen and U. P. Svensson, *"Performance of some linear time-varying systems in control of acoustic feedback"*, Journal of the Acoustical Society of America, vol. 106, no. 1, 1999.

[4] K. Kobayashi, K. Furuya and A. Kataoka, *"An adaptive microphone array for howling cancellation"*, Acoustical Science & Technology, vol. 24, no 1, 2003.

[5] W. Leotwassana, R. Punchalard and W Silaphan, *"Adaptive Howling Canceller using Adaptive IIR Notch Filter: Simulation and Implementation"*, IEEE Int. Conf. Neural Networks & Signal Processing, Nanjing, China, December 2003.

[6] T. van Waterschoot, G. Rombouts and Marc Moonen, *"On the performance of decorrelation by prefiltering for adaptive feedback cancellation in Public Address systems"*, Proceedings of the 2004 IEEE Benelux Signal Processing Symposium (SPS 2004), Hilvarenbeek, the Netherlands, April 15-16 2004, pp. 167-170.

[7] Jorge Leitão, Gabriel Fernandes and Aníbal Ferreira, *"Adaptive Room Equalization in the Frequency Domain"*, 116th AES Convention Paper, Berlin, Germany, May 2004.

[8] Simon Haykin, *Adaptive Filter Theory*, 4th. Edition, Prentice-Hall International, September 2001.

[9] Texas Instrument, Dallas, *TX, TMS320 C6000 CPU and Instruction Set*, 2000, SPRU189F.

[10] John G. Proakis, Dimitris Manolakis, *Digital Signal Processing: Principles, Algorithms and Applications*, 3rd. Edition, Prentice-Hall International, October 1995.

[11] Ann Spriet, *"Adaptive Filter Techniques for Noise Reduction and Acoustic Feedback Cancellation in Hearing Aids"*, PhD Thesis, Katholieke Universiteit Leuven, Belgium, 2004.

[12] H. Chi, S. Gao, S. Soli and A. Alwan, *"Band-Limited Feedback Cancellation with a Modified Filtered-X LMS Algorithm for Hearing Aids"*, Speech Communication 39 (2003) 147-161, Elsevier Science B.V.

[13] J. A. Maxwell and P. M. Zurek, *"Reducing Acoustic Feedback in Hearing Aids"*, IEEE Transactions on Speech and Audio Processing, vol. 3, no. 4, July 1995.

[14] Aníbal Ferreira, *"Accurate Estimation in the ODFT Domain of the Frequency, Phase and Magnitude of Stationary Sinusoids"*, 2001 Workshop on Applications of Signal Processing to Audio and Electro-acoustics, New Paltz, New York, October 21-24, 2001.